Environ. Sci. Technol. **2010,** *44,* 3324–3331

Temperature Sensitivity of Black Carbon Decomposition and Oxidation

BINH THANH NGUYEN,[†,‡] JOHANNES LEHMANN,[*,†] WILLIAM C. HOCKADAY,[§] STEPHEN JOSEPH,[⊥] AND CAROLINE A. MASIELLO[§]

Department of Crop and Soil Sciences, Cornell University, Ithaca, New York 14853, University of New South Wales, Sydney NSW 2251, Australia, and Department of Earth Science, Rice University, Houston, Texas 77251

Received October 10, 2009. Revised manuscript received March 23, 2010. Accepted March 31, 2010.

Global warming accelerates decomposition of soil organic carbon (SOC) pools with varying rates and temperature sensitivities. Black carbon (BC) materials are among the slowest decomposing components of the SOC pool. Although BC is a large component of SOC in many systems, the influence of temperature on decomposition of BC bearing different chemical and physical structures remains poorly understood. Four BC materials, produced by carbonizing corn residue and oak wood at 350 and 600 °C (corn-350-BC, corn-600-BC, oak-350-BC, and oak-600-BC), were mixed with pure sand and incubated at 4, 10, 20, 30, 45, and 60 °C for 1 year. Corn-BC was more porous than oak-BC as determined by scanning electron microscopy (SEM). Increasing the charring temperature from 350 to 600 °C led to greater aromaticity with 5−15% more C in aromatic rings and a 39−57% increase in both nonprotonated aromatic C and aromatic bridgehead C quantified by nuclear magnetic resonance (NMR) spectroscopy and a greater degree of order and development of C layers as observed by transmission electron microscopy (TEM). With a temperature increase from 4 to 60 °C, C loss of corn-350-BC increased from 10 to 20%, corn-600-BC, from 4 to 20%, oak-350-BC, from 2.3 to 15%, and oak-600-BC from 1.5 to 14% of initial C content, respectively. Temperature sensitivity (Q_{10}) decreased with increasing incubation temperature and was highest in oak-600-BC, followed by oak-350-BC, corn-600-BC, and corn-350-BC, indicating that decomposition of more stable BC was more sensitive to increased temperature than less stable materials. Carbon loss and potential cation exchange capacity (CECp) significantly ($p < 0.05$) correlated with O/C ratios and change in O/C ratios, suggesting that oxidative processes were the most important mechanism controlling BC decomposition in this study.

Introduction

The temperature sensitivity of the decomposition (here synonymous with mineralization and C loss) of resistant soil C pools is still under debate. A number of studies report increasing sensitivity of stable soil organic carbon (SOC) to warming, relative to young and labile SOC pools (*1*−*4*). Conversely, Liski et al. (*5*) concluded that in response to warming, decomposition of the resistant SOC pool was less sensitive than that of labile pools and Giardina and Ryan (*6*) even reported that decomposition of SOC in forest mineral soil was not influenced by increased temperature.

These apparent discrepancies may be explained by variation in soil characteristics that limit decomposer access to SOC, e.g. the formation of aggregates or organo−mineral interactions (*3*). Since decomposers' access to SOC is less affected by temperature than microbial metabolism on the short-term (*3*), warming may not increase decomposition when the physical protection of SOC is significant.

In addition to physical protection, chemical recalcitrance influences SOC decomposition rates. Black carbon (BC) is a highly recalcitrant form of C in soils and accounts for a considerable proportion of SOC, for example up to 45% (by mass) in German Chernozemic soils (*7, 8*), up to 35% in a range of US agricultural soils (*9*), and on average 20% for a continental-scale analysis of Australian soils (*10*). BC was estimated to have mean residence times of a thousand years or more in soil (*10*−*12*). In contrast to non-BC organic matter in soils, the highest proportion of BC occurs in the light fraction (*13*), rather than the mineral-bound fraction of SOC. Therefore, the temperature sensitivity of BC may be largely controlled by its intrinsic chemical recalcitrance rather than physical protection.

In addition, BC materials greatly differ in chemical, physical, and structural properties and therefore stability against decomposition, depending on production temperature and BC precursor material (*14*). BC is the product of incomplete combustion of vegetation (*15*) and has a high degree of aromaticity (*16, 17*). The defining feature of BC is an elevated elemental C content from condensed aromatic rings (*18*), having both microcrystalline graphitic structure (*19*) as well as amorphous nonorganized structure (*20*). With increasing charring temperature, polyaromatic sheets, composed of basic aromatic units, partly stack over each other (*21*), forming three-dimensional structures and very heterogeneous particles (*22*). BC stability is likely determined by both chemical forms and micro- and nanostructural physical characteristics. The temperature sensitivity of decomposition is thought to increase with greater recalcitrance (*3*). How sensitively BC materials with differing properties respond to a warming environment has not yet been quantified.

While warming typically increases microbial activity, individual microbial communities have a specific temperature range over which the SOC decomposition rate is optimized (*23*). Several authors show a link between BC degradation and microbial activity (*24*−*26*). However, abiotic oxidation of BC (*20*) is also accelerated by the increase in temperature. Cheng et al. (*27*) reported a higher O content when BC particles were incubated at 70 °C than at 30 °C after gamma irradiation, indicating that BC oxidation may occur abiotically beyond the optimum generally considered for microbial activity. The same authors (*28*) observed a significant positive correlation between the formation of oxygen functional groups on BC and increasing mean annual

* To whom correspondence should be addressed. Phone: (607) 254-1236. Fax: (607) 255-3207. E-mail: CL273@cornell.edu.
† Cornell University.
‡ Current address: Rubber Research Institute of Vietnam, 301 Nguyen Van Troi, Tan Binh, Ho Chi Minh City, Vietnam.
§ Rice University.
⊥ University of New South Wales.

10.1021/es903016y

Published on Web 04/12/2010

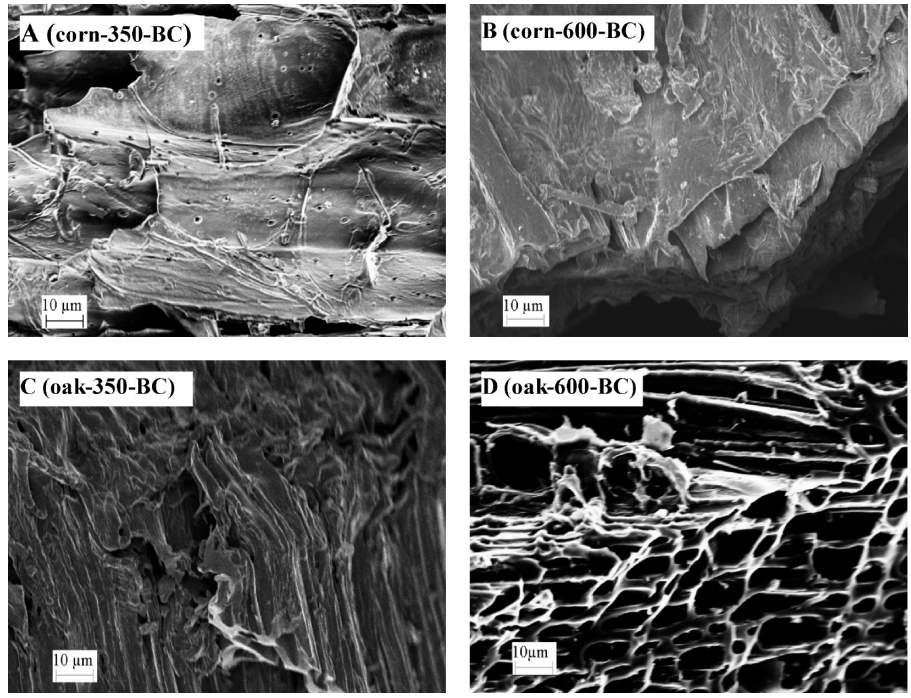

FIGURE 1. SEM images showing the morphology of BC materials: (A) corn at 350 °C, (B) corn at 600 °C, (C) oak at 350 °C, and (D) oak at 600 °C. A and D are images capturing cross sections whereas B and C are derived from a longitudinal section of the materials at the same magnification of 1 K. See Figure S1a and b of the Supporting Information for additional SEM images.

temperature. Therefore, it is not clear whether an optimum also exists for BC decomposition.

To address these knowledge gaps, this study investigates the effects of temperature on decomposition of BC materials with contrasting recalcitrance to test the hypotheses that (a) decomposition rates of BC increase with higher incubation temperature and (b) decomposition of more stable BC materials characterized by greater abundance of condensed aromatic C is more sensitive to increased temperature than that of less stable BC materials.

Materials and Methods

Experiment. Four BC materials (corn-350-BC, corn-600-BC, oak-350-BC, and oak-600-BC) were produced by carbonizing total corn crop residue (*Zea mays* L.) and wood shavings of oak (*Quercus* ssp.) at 350 and 600 °C using slow pyrolysis (*29*). Details of methods as well as initial chemical characteristics are described in the Supporting Information. In brief, all BC materials were incubated in sand culture at six different temperatures using eight replicates. Carbon loss, contents of N, H, O, and CECp (potential cation exchange capacity) were determined after 1 year as described in the Supporting Information.

Microstructures of the BC particles were investigated using a LEO (ZEISS) 1550 scanning electron microscope (SEM). The sample particles were mounted on an aluminum stub and were coated with carbon. Because the particles were thick and presented with features on the micrometer scale, the coating material did not interfere with the scanned images.

Transmission electron microscopy (TEM) images of BC particles were collected using a FEI Tecnai T12 Spirit Twin TEM/STEM at 120 kV (5350 NE Dawson Creek Drive Hillsboro, Oregon). The materials were finely ground (*30*), suspended in ethanol, briefly sonicated (*31*), and deposited on a Lacey carbon-coated copper grid.

Functional group chemistry of the initial BC was determined by direct polarization (DP-) ^{13}C NMR spectroscopy. The average size of aromatic domains, number of oxygen atoms and alkyl side chains attached to each cluster, and average length of the side chains were calculated as described in the Supporting Information.

Statistical Analysis. Analysis of variance (ANOVA) was applied using a completely randomized factorial design with eight replicates and three experimental factors. A student test was used to classify any significant difference in means between treatments. All statistical analyses and model fitting were done with JMP software 6.0, Sigma plot 11, and Microsoft Excel.

Results

Microstructure of BC. The SEM images reflect representative parts of BC from both corn residue and oak wood used in this study (Figure 1). The plant cell structure of the original biomass materials was clearly visible for the BC particles formed at both 350 and 600 °C. At the microscale, corn-BC appeared more porous than oak-BC and the cell walls of corn-BC were thinner than that of oak-BC.

Nanostructure of BC. In general, oak-BC showed slightly more parallel orientation of C layers than corn-BC (Figure 2) at both production temperatures. Corn-350-BC was composed of short C layers, which arranged rather randomly, forming an amorphous structure (Figure 2A). In contrast, parts of oak-350-BC tended to include circular C structures with a diameter of less than 1 nm (Figure 2C). Parallel arrangement of 3−5 C layers formed slightly curved shapes in corn-600-BC with an interlayer spacing of 0.38−0.41 nm (Figure 2B) whereas oak-600-BC may include weak lattice structures (Figure 2D). Increasing carbonization temperature led to slightly better ordered C layers and elongation of C layers for both types of BC, though amorphous C structures prevailed. Corn-BC appeared to show a greater increase in C layer orientation when pyrolysis temperature was increased compared to oak-BC.

Functional Group Chemistry and Structure of BC Materials. Aromaticity increased from 83−86% to 90−94% when charring temperature was increased from 350 to 600 °C, with 5−15% more C in aromatic rings (Table 1 and Figure S3). Conversely, total aliphatic C was higher in materials formed at the lower charring temperature. Non-

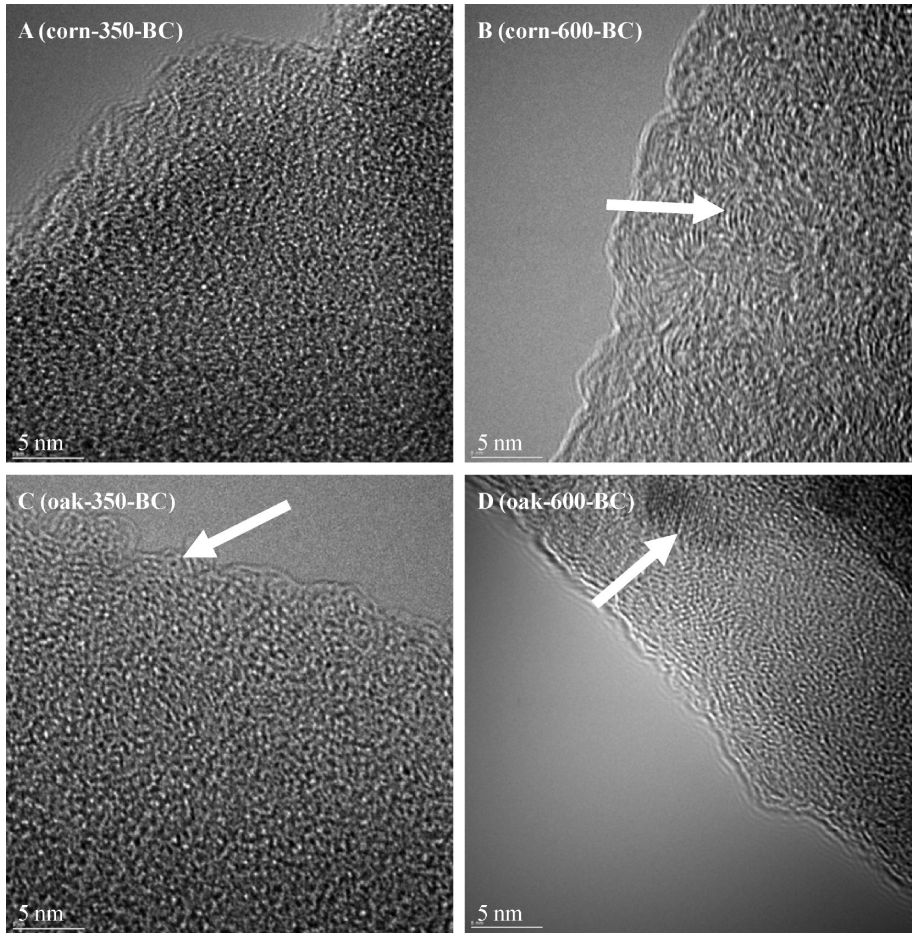

FIGURE 2. TEM images of the BC materials. The arrow in panel B indicates an oval shape of a size of a few nanometers formed by curling of C layers. The arrows in the panels indicate features discussed in the text. See Figure S2a and b of the Supporting Information for additional images.

TABLE 1. Relative Proportion (percent of BC-C) of Chemical Functional Groups of BC Determined by DP ^{13}C NMR

	corn-350-BC	corn-600-BC	oak-350-BC	oak-600-BC
carbon functional groups (measured)				
total aromatic C (>95 ppm)	83.0	94.1	85.9	90.2
aromatic C in rings	76.9	88.2	82.8	86.6
carbonyl (>165 ppm)	6.1	5.9	3.1	3.6
protonated aromatic C	17.6	3.3	29.0	5.7
nonprotonated aromatic C	59.3	84.9	53.8	84.5
phenolic or aromatic ether (145−165 ppm)	6.4	7.3	11.4	9.5
aromatic bridgehead C	44.2	61.3	42.4	59.0
total alkyl C (<95 ppm)	17.0	5.9	14.1	6.2
carbon structural properties (calculated)				
ave number of aromatic C per cluster	19	40	18	37
ave number of oxygen attachments per cluster	1.6	3.3	2.5	3.9
ave number of alkyl attachments per cluster	2.2	7.4	2.7	6.6
ave number of alkyl C per side chain	1.9	0.4	1.1	0.4
total C observed (spin counting, ±10)	110	91	104	98

protonated aromatic C increased by 43−57%, and aromatic bridgehead C by 39% with increasing charring temperature. At 600 °C, aromatic clusters contained on average 38−40 aromatic C atoms with 4 out of 7 linkages to neighboring clusters (Figure S4). At 350 °C, cluster sizes were only 19 aromatic C atoms large with two links to neighboring clusters.

BC Mineralization. BC was mineralized to a greater extent when incubation temperature was increased from 4 to 30 °C, at which C loss was 4.6% and 14.6%, respectively (data calculated, based on the fitted model). Remaining C (percent of initial C) of corn-BC was significantly lower than that of oak-BC, and remaining C of 350-BC was significantly lower than that of 600-BC at any incubation temperature (Figure 3B). The change of BC mineralization as a function of incubation temperature significantly depended on BC types. For example, the temperature sensitivity of corn-600-BC from 4 to 30 °C incubation temperature was greater than that of corn-350-BC (Figure 3B).

On the basis of the fitted model (Supporting Information Table S2), corn-BC lost more C per degree Celsius increase in incubation temperature (parameter b) compared to oak-BC. The fitted model also showed that b (rate of C loss per

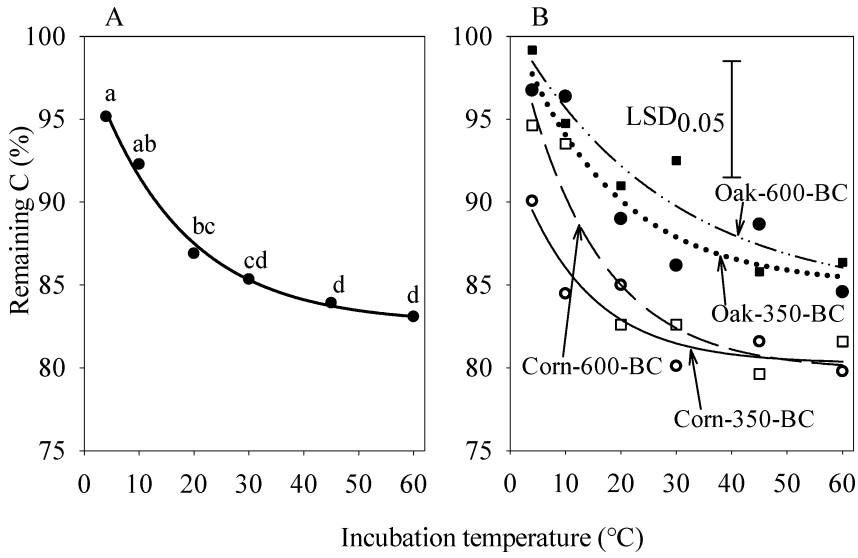

FIGURE 3. Remaining C of overall mean (A) and individual BC materials (B) after the first year of incubation. Within panel A, data points with the same letter were not significantly different. Parameters of the fitted curves are shown in Supporting Information Table S2. See Tables S3 and S4 for individual remaining C values in the Supporting Information.

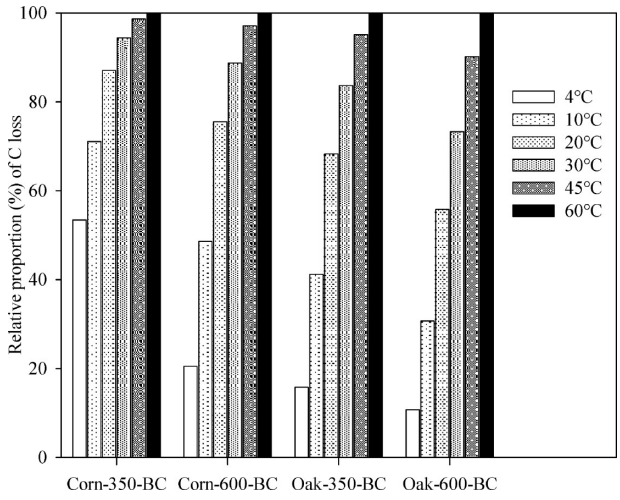

FIGURE 4. Proportion of C loss of the BC materials at different temperatures relative to that at 60 °C.

increase in °C incubation temperature) decreased with increasing charring temperature. We conclude from this that incubation temperature had a lower influence on absolute C loss of the more structurally ordered BC materials such as oak-BC and BC produced at higher charring temperature.

The C loss of corn-350-BC, incubated at 4 °C, was as much as 53% of that incubated at 60 °C, followed by corn-600-BC (21%), oak-350-BC (16%) and then oak-600-BC (11%) (Figure 4). Increasing the incubation temperature resulted in different increases in the proportion of C loss, depending on temperature ranges and BC materials. The greatest increase in C loss of approximately 25−28% was similar for corn-600-BC and oak-350-BC, when increasing the incubation temperature from 4 to 10 °C and from 10 to 20 °C.

Oxygen Content and CEC. With increasing incubation temperature, the O/C ratios increased and a first order model was a good fit ($r^2 = 0.96$) to the data points (Figure 5A). At temperatures higher than 10 °C, the O/C ratios of the 4 BC materials after incubation were significantly greater than before incubation. Relative increases in O/C ratios as a function of incubation temperature were significant ($P < 0.05$) and similar among the four BC materials. However, the absolute values of O/C ratios were highest in corn-350-BC,

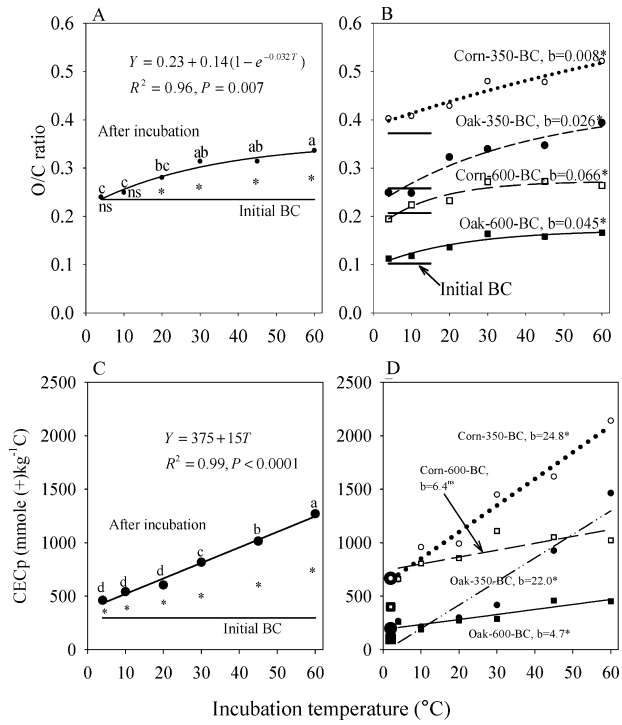

FIGURE 5. O/C ratios as well as CECp of overall means (A and C) and individual BC materials (B and D). Within panels A and C, data points with the same letter are not significantly different. *b* is the slope of the fitted curve. * and ns indicate whether the slope or the difference in O/C ratios or CECp after and before incubation is significant ($P < 0.05$) or nonsignificant ($P > 0.05$), respectively. See Supporting Information Tables S5 and S6 for individual O/C values and Tables S7 and S8 for individual CECp values.

followed by corn-600-BC, oak-350-BC, and oak-600-BC at any incubation temperatures (Figure 5B).

The CECp as an indicator of surface charge developed through oxidation of BC surfaces increased significantly from 808 to 973 mmol kg^{-1} C when the incubation temperature was increased from 4 to 60 °C (Figure 5C). The increase in CECp as a function of incubation temperature greatly depended on the charring temperatures. CECp of corn-BC and oak-BC formed at 350 °C changed with a rate of 25 and

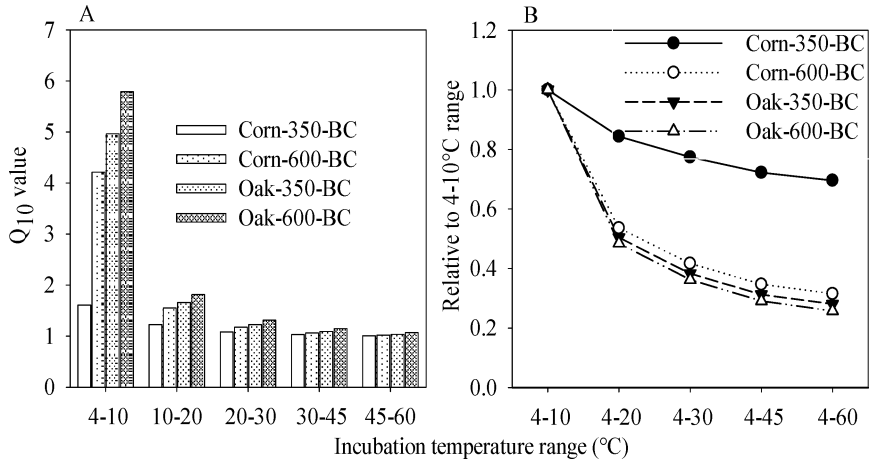

FIGURE 6. Absolute Q_{10}values of BC materials at different ranges of incubation temperature (A) and Q_{10} relative to that at the 4−10 °C range (B). These values were calculated based on Supporting Information eq S5.

22 mmol (+) kg^{-1} C $°C^{-1}$, respectively, much greater than the materials formed at 600 °C with a rate of 6.4 and 4.7 mmol (+) kg^{-1} C $°C^{-1}$ for corn-600-BC and oak-600-BC, respectively (Figure 5D). CECp of corn-BC was significantly greater than that of oak-BC at any charring temperature and incubation temperature.

With increasing O/C ratios, the remaining C (%) significantly decreased and CECp (mmol (+) kg^{-1} C) increased ($P < 0.001$; Supporting Information Figure S5A). Changes in O/C ratios were also significantly and inversely correlated with the remaining C content and positively with change in CECp ($P < 0.001$; Supporting Information Figure S5B).

Temperature Coefficient (Q_{10}). The Q_{10} is a quantitative measure of the temperature sensitivity and describes a relative increase in decomposition with warming. In the lowest temperature range from 4 to 10 °C, the Q_{10} value of corn-350-BC, 1.6, was much smaller than those of the other BC materials, varying from 4.2 to 5.8 (Figure 6A). At higher temperature ranges, the difference in Q_{10} between the four BC materials decreased, varying from 1.01 to 1.82, with corn-350-BC still having the lowest and oak-600-BC the highest. Relative to the Q_{10} at 4−10 °C, the Q_{10} values of corn-350-BC decreased to a lesser extent with increasing incubation temperature ranges than those of the other materials (Figure 6B).

Discussion

BC Properties. The chemical, physical and structural properties of BC were greatly influenced by production temperature and biomass type confirming earlier studies (*32*−*34*). With increasing production temperature, BC materials tended to condense and increase in aromaticity (*35*), confirmed by our NMR analyses. Nishimiya et al. (*32*) also observed an increased condensation of aromatic rings as production temperature was increased to 2000 °C. Similarly, nonprotonated aromatic C increased indicating a significant increase in the average number of fused aromatic C which comprises the BC backbone structure (Table 1).

An important difference between corn-BC and oak-BC was observed in their microstructure (Figure 1). The SEM images captured from corn and oak materials formed at 350 and 600 °C showed that the tissue structure of the original plant biomass was retained in the BC materials which showed thicker wall structures in oak than corn, in agreement with observations by Brodowski et al. (*36*) and Kim and Hanna (*37*).

At the nanoscale, the C morphology of BC materials has been characterized by different models, such as a diamond structure (*38*), onionlike structure (*39*), fullerene structure (*40*), ribbonlike structure (*41*), and randomly ordered strip segment structures (*42*). Although a BC particle may bear various nanostructures, C morphology of 600-BC in this study may have included structures similar to a model by Franklin (*42*) for nongraphitizing C, while that of 350-BC was dominantly amorphous in structure. In general, amorphous structures were dominant (Figures 2A and C). However, some ordered parallel structures (Figure 2D), in some cases including onionlike forms possibly of fullerene type (Figure 2B), were also visible. Bourke et al. (*19*) did not find fullerene structures in a range of BC materials using matrix-assisted, laser desorption ionization coupled with time-of-flight mass spectroscopy, which suggests further investigation is needed to fully identify the slightly ordered structures observed in our study.

The effect of charring temperature has been reported to include (a) thermal breaking of cross-links connecting crystallite planes and (b) gradual movement of a whole plane or a group of planes (*42*) for a parallel rearrangement of C layers. In accordance with this observation, BC formed at 600 °C in our study resulted in larger clusters sizes (Table 1), with an indication of more parallel arrangement than at 350 °C (Figure 2). A greater proportion of aromatic C in rings (Table 1) and an indication of slightly greater ordering in C layers of oak-350-BC (Figure 2C) than corn-350-BC (Figure 2) did not lead to an increased degree of aromatic C (Table 1) or parallel ordering of C layers in oak-600-BC (Figure 2D) than in corn-600-BC (Figure 2B). Rather a greater change in nanostructures was observed in corn-BC than in oak-BC as a result of increased charring temperature (Figure 2). Whether this is a result of the C forms of the biomass or the amount and type of minerals present requires further investigation.

Regardless of biomass type, the segments of C layers may first be thermally separated (*42*) during pyrolysis and move closer to each other, forming nanoparticles (*30*), or even join together, generating longer C layer segments observed at temperatures above 1000 °C. At our much lower temperatures, a lengthening of C layers can be qualitatively identified, appearing in strip segments with higher production temperature (Figure 2, comparable to the work of Kercher and Nagle (*21*)). Consequently, C concentrations were greater (Supporting Information Table S1) and clusters were larger (Table 1) combined with a tendency toward more parallel structures in 600-BC than in 350-BC (Figure 2).

BC Mineralization and Temperature Sensitivity. The experimentally obtained values of temperature sensitivity in this study varied from 1.01 to 5.79 and are consistent with Q_{10} ranges from 1 to 8, calculated through CO_2 evolution from incubated soils (*43*). In addition, Q_{10} calculated for the

temperature range from 5 to 15 °C in this study was comparable to that of about 3.4, reported by Cheng et al. (*12*) for hard wood-derived BC. For temperatures between 4 and 10 °C, Q_{10} values of BC materials in this study ranged from 1.6 to 5.7 and decreased rapidly with increasing incubation temperature, resulting in lower differences in Q_{10} values between materials at high incubation temperatures. This is consistent with previous studies showing that the temperature coefficient of organic matter decomposition is not constant but rather decreases as temperature increases (*3, 43, 44*).

On the basis of Q_{10} values (Figure 6) decomposition of more stable BC materials, such as oak-BC formed at 600 °C increased to a greater extent as a result of increased incubation temperature than that of more labile BC materials, such as corn-BC formed at 350 °C. This finding is in agreement with other authors (*1*−*3*), who hypothesized that the mineralization of the resistant SOC fraction would be more sensitive to temperature increases than that of labile SOC. Likewise, Fierer et al. (*45*) observed that decomposition of poorer-quality litter was more sensitive to temperature increases than that of better-quality matter. Recently Conant et al. (*46*) also reported a rise in temperature sensitivity of soil C decomposition upon depletion of soil labile C.

However, other studies demonstrated different results. Fang et al. (*47*) and Czimczik and Trumbore (*48*) found the same mineralization rates of labile and resistant SOC pools with increased temperature, based on an incubation experiment. Similarly, Reichstein et al. (*49*) showed no difference in Q_{10} values of SOC in organic and mineral horizons. These differences to experiments showing increased temperature sensitivity with lower C quality were explained by invoking resource limitation due to aggregation or organo−mineral interactions (*3*). This was not the case in our incubation studies that were conducted in a sand medium.

More labile BC materials (corn-BC) showed a greater response in absolute C loss, however, to a rise in incubation temperature than oak-BC at the same temperature range. This stands in contrast to the greater relative temperature sensitivity of the more stable oak-BC, as described above using the Q_{10} values. This is a result of how Q_{10} values are obtained. With a low mineralization rate at low temperatures (as is the case with the more stable oak-BC), even a small increase in C loss as a result of a temperature increase would result in a large Q_{10} value and vice versa.

The easily decomposing fraction of corn-350-BC was most sensitive at lowest incubation temperatures (4−10 °C), while corn-600-BC and oak-350-BC were most sensitive to temperature changes from 10 to 20 °C and oak-600-BC had the highest portion of C loss at 20 °C (Figure 4). As a result, it may be assumed that the BC materials may be composed of different fractions, which differed in their response to temperature changes. The least stable fraction, which was decomposable even at a low temperature of 4 °C, was significantly more abundant in corn-350-BC than in the other materials. This fraction accounted for about 53% of the total C loss of corn-350-BC during the first year of incubation. The most labile fraction at temperatures from 10−20 °C was found to the greatest extent in corn-600-BC and oak-350-BC, accounting for 25−27% of total C loss. The stable fraction, decomposable to the greatest extent at 20 °C, was most abundant in oak-600-BC, accounting for 25% of the mineralized fraction of the material. The BC fraction that decomposed at the lowest incubation temperature likely contains mostly labile compounds, such as alkyl C (Table 1). The fraction that disappeared at higher incubation temperatures increasingly contains aromatic compounds, which are more resistant to decomposition. This has to be considered when interpreting the Q_{10} and absolute decomposition rates at different incubation temperatures.

BC Decomposition Mechanisms. We observed a significant relationship between O/C ratio or change in O/C ratio and remaining C (Supporting Information Figure S5). This indicates that the major mechanism mineralizing the studied BC involved formation of oxygen functional groups (some oxygen adsorption may also play a role (*27*)) which confirms earlier conclusions by others (*20, 27*).

With an increase in incubation temperature from 5 to 30 °C, mineralization of SOC typically shows an exponential increase (*50*), whereas at greater temperatures often decreases in mineralization are observed (*23*). In contrast, we observed a continued slight increase in C loss at incubation temperatures higher than 30 °C, suggesting that abiotic oxidation to carbon dioxide likely occurred in addition to microbial decomposition and may have been dominant at temperatures above 30 °C (we did not distinguish abiotic and biotic C loss in this experiment). The importance of microbial decay may have decreased with a rise in incubation temperature as shown by Cheng et al. (*27*).

The micro- and nanostructure of BC is likely important for determining BC stability, as decomposition first occurs at accessible sites such as particle surfaces (*23, 51, 52*). This may also apply to the edge of individual C layers or to sites of defect structures in C layers. According to Pierson (see ref *53*, p 63), this is due to the greater energy state at the edges of a layer or at the ends of basal layers than in the basal plane. Apart from greater mineralization reactions, the materials having more active sites may also interact to a greater extent with soil minerals, resulting in better protection of BC from further formation of oxygen functional groups and mineralization. However, BC in this study was mixed with pure sand material; therefore, such protecting mechanisms are likely negligible.

The chemical recalcitrance of these nanocomposites is also a function of the way in which the C−C bonds are arranged. Corn-BC produced at low charring temperature had a less ordered structure resembling amorphous C (Figure 2) with lower cluster sizes (Table 1), which likely had a high quantity of reactive sites, and thereby a low stability. In contrast, the BC produced at higher temperature (especially oak-BC) appeared to show a slightly greater degree of order and larger clusters with greater number of side chains directly linked to neighboring aromatic clusters, which may explain the increased stability by a reduction of active sites for formation of oxygen functional groups and decomposition. An increase of internal surface area through a less ordered structure (*54*) may also decrease its stability. In accordance with our results, increasing charring temperature typically shows longer crystallite sizes (*35*) which even further reduces the number of active sites (see ref *53*, p 64). However, perfect layers of graphene sheets in graphite are held together by comparatively weak van-der-Waals forces, whereas unordered turbostratic C or even folded fullerene structures are much more stable (*54*).

In addition to the C structure itself, nutrient contents may also affect BC mineralization. We observed a higher content of N, K, and Ca in corn-BC than in oak-BC (Supporting Information Table S1 and ref *29*). In fact, Fierer et al. (*5*) reported a great increase in CO_2 release in subsurface soil but negligible change in surface soil as a consequence of N and P addition and they attributed the influence of N and P addition to an enhanced production of enzymes required for C mineralization in the nutrient-limited environment.

Overall, the decomposition over the 1-year period appears to be high and may be the result of rapid decay of the easily decomposable fraction of BC as discussed in more detail elsewhere (*29*). A rate of decay can not be calculated with one data point used in our study, and it is not possible to

predict from our assessment whether the remaining BC will continue to decompose or persist.

BC oxidation did not only lead to C loss, but also to an increase in negative surface charge (CECp) likely through formation of carboxylic groups by oxidation (*27*) on the edges of the aromatic backbone as hypothesized by Glaser et al. (*56*). Liang et al. (*57*) confirmed that oxidation of BC was the main reason for the high CEC of Anthrosols from the Brazilian Amazon. In this study we also observed a significant relationship ($R^2 = 0.58$; $P < 0.001$) between O/C ratios and CECp or between the change in O/C ratios and the change in CECp (Supporting Information Figure S5), indicating the importance of the formation of oxygen functional groups in enhancing total negative charge of BC.

In summary, the BC structure and properties were significantly controlled by charring temperature and biomass type, which in turn changed the temperature sensitivity of decomposition. The relative importance of the BC structure at the micro- and nanoscale, in comparison to the role of minerals, such as N and K, for BC mineralization is still poorly understood and requires studies using BC materials controlled for structure and mineral content. Because the studied BC types contained fractions differing in stability, determination of Q_{10} values from fresh BC may interfere with the changes in properties during incubation. Therefore, studies of temperature sensitivity targeting aged BC are needed in addition to those of fresh BC.

Acknowledgments

Financial support from the Vietnam Education Foundation (VEF) and the Wu Fellowship for B.T.N. is gratefully acknowledged. This work was funded in part by a USDA−Hatch and a NYSERDA grant. Any opinions, findings, and conclusions or recommendations expressed in this material are those of the authors and do not necessarily reflect the views of the funding agencies. Many thanks to Kelly Hanley for invaluable help during the experiment, to John Grazul and John Hunt for TEM and SEM image collection, and to BEST Energies for supplying the BC. The first author is also grateful to the Rubber Research Institute of Vietnam (RRIV) for support.

Supporting Information Available

SEM images (Figure S1a and b), TEM images (Figure S2a and b), DPMAS ^{13}C NMR spectra (Figure S3), proposed structural information (Figure S4), regression between C loss and oxidation (Figure S5), bulk chemical properties (Table S1), regression results (Table S2), remaining C values and ANOVA (Tables S3 and S4), O/C ratio and ANOVA (Tables S5 and S6), CECp and ANOVA (Tables S7 and S8). This material is available free of charge via the Internet at http://pubs.acs.org/.

Literature Cited

(1) Agren, G. I. Temperature dependence of old soil organic matter. *Ambio* **2000**, *29*, 55–55.
(2) Knorr, W.; Prentice, I. C.; House, J. I.; Holland, E. A. Long-term sensitivity of soil carbon turnover to warming. *Nature* **2005**, *433*, 298–301.
(3) Davidson, E. A.; Janssens, I. A. Temperature sensitivity of soil carbon decomposition and feedbacks to climate change. *Nature* **2006**, *440*, 165–173.
(4) Reichstein, M.; Kätterer, T.; Andren, O.; Ciais, P.; Schulze, E. D.; Cramer, W.; Papale, D.; Valentini, R. Does the temperature sensitivity of decomposition of soil organic matter depend upon water content, soil horizon, or incubation time. *Biogeosciences* **2005**, *2*, 317–321.
(5) Liski, J.; Ilvesniemi, H.; Makela, A.; Westman, C. J. CO_2 emissions from soil in response to climatic warming are overestimated - The decomposition of old soil organic matter is tolerant of temperature. *Ambio* **1999**, *28*, 171–174.
(6) Giardina, C. P.; Ryan, M. G. Evidence that decomposition rates of organic carbon in mineral soil do not vary with temperature. *Nature* **2000**, *404*, 858–861.
(7) Schmidt, M. W. I.; Skjemstad, J. O.; Gehrt, E.; Kögel-Knabner, I. Charred organic carbon in German chernozemic soils. *Eur. J. Soil Sci.* **1999**, *50*, 351–365.
(8) Schmidt, M. W. I.; Skjemstad, J. O.; Jäger, C. Carbon isotope geochemistry and nanomorphology of soil black carbon: Black chernozemic soils in central Europe originate from ancient biomass burning. *Global Biogeochem. Cycles* **2002**, *16*, GB1123.
(9) Skjemstad, J. O.; Reicosky, D. C.; Wilts, A. R.; McGowen, J. A. Charcoal carbon in U.S. agricultural soils. *Soil Sci. Soc. Am. J.* **2002**, *66*, 1249–1255.
(10) Lehmann, J.; Skjemstad, J. O.; Sohi, S.; Carter, J.; Barson, M.; Falloon, P.; Coleman, K.; Woodbury, P.; Krull, E. Australian climate-carbon cycle feedback reduced by soil black carbon. *Nature Geosci.* **2008**, *1*, 832–835.
(11) Swift, R. S. Sequestration of carbon by soil. *Soil Sci.* **2001**, *166*, 858–871.
(12) Cheng, C. H.; Lehmann, J.; Thies, J. E.; Burton, S. D. Stability of black carbon in soils across a climatic gradient. *J. Geophys. Res.-Biogeosci.* **2008**, *113*, G02027.
(13) Glaser, B.; Balashov, E.; Haumaier, L.; Guggenberger, G.; Zech, W. Black carbon in density fractions of anthropogenic soils of the Brazilian Amazon region. *Org. Geochem.* **2000**, *31*, 669–678.
(14) Labbe, N.; Harper, D.; Rials, T. Chemical structure of wood charcoal by infrared spectroscopy and multivariate analysis. *J. Agric. Food Chem.* **2006**, *54*, 3492–3497.
(15) Koelmans, A. A.; Jonker, M. T. O.; Cornelissen, G.; Bucheli, T. D.; Van Noort, P. C. M.; Gustafsson, O. R. Black carbon: The reverse of its dark side. *Chemosphere* **2006**, *63*, 365–377.
(16) Kuhlbusch, T. A. J. Method for determining black carbon in residues of vegetation fires. *Environ. Sci. Technol.* **1995**, *29*, 2695–2702.
(17) Haumaier, L.; Zech, W. Black carbon - possible source of highly aromatic components of soil humic acids. *Org. Geochem.* **1995**, *23*, 191–196.
(18) Kim, S.; Kaplan, L. A.; Benner, R.; Hatcher, P. G. Hydrogen-deficient molecules in natural riverine water samples—evidence for the existence of black carbon in DOM Marine. *Chemistry* **2004**, *92*, 225–234.
(19) Bourke, J.; Manley-Harris, M.; Fushimi, C.; Dowaki, K.; Nunoura, T.; Antal, M. J. Do all carbonized charcoals have the same chemical structure? 2. A model of the chemical structure of carbonized charcoal. *Ind. Eng. Chem. Res.* **2007**, *46*, 5954–5967.
(20) Cohen-Ofri, I.; Popovitz-Biro, R.; Weiner, S. Structural characterization of modern and fossilized charcoal produced in natural fires as determined by using electron energy loss spectroscopy. *Chem.—Eur. J.* **2007**, *13*, 2306–2310.
(21) Kercher, A. K.; Nagle, D. C. Microstructural evolution during charcoal carbonization by X-ray diffraction analysis. *Carbon* **2003**, *41*, 15–27.
(22) Schmidt, M. W. I.; Noack, A. G. Black carbon in soils and sediments: Analysis, distribution, implications, and current challenges. *Global Biogeochem. Cycles* **2000**, *14*, 777–793.
(23) Qureshi, S.; Richards, B. K.; McBride, M. B.; Baveye, P.; Steenhuis, T. S. Temperature and microbial activity effects on trace element leaching from metalliferous peats. *J. Environ. Qual.* **2003**, *32*, 2067–2075.
(24) Brodowski, S. B. Origin, function, and reactivity of black carbon in the arable soil environment. Ph.D. Dissertation, University of Bayreuth, Bayreuth, Germany, 2004.
(25) Hamer, U.; Marschner, B.; Brodowski, S.; Amelung, W. Interactive priming of black carbon and glucose mineralization. *Org. Geochem.* **2004**, *35*, 823–830.
(26) Marschner, B.; Brodowski, S.; Dreves, A.; Gleixner, G.; Gude, A.; Grootes, P. M.; Hamer, U.; Heim, A.; Jandl, G.; Ji, R.; Kaiser, K.; Kalbitz, K.; Kramer, C.; Leinweber, P.; Rethemeyer, J.; Schaeffer, A.; Schmidt, M. W. I.; Schwark, L.; Wiesenberg, G. L. B. How relevant is recalcitrance for the stabilization of organic matter in soils. *J. Plant Nutr. Soil Sci.* **2008**, *171*, 91–110.
(27) Cheng, C. H.; Lehmann, J.; Thies, J. E.; Burton, S. D.; Engelhard, M. H. Oxidation of black carbon by biotic and abiotic processes. *Org. Geochem.* **2006**, *37*, 1477–1488.
(28) Cheng, C. H.; Lehmann, J.; Engelhard, M. H. Natural oxidation of black carbon in soils: Changes in molecular form and surface charge along a climosequence. *Geochim. Cosmochim. Acta* **2008**, *72*, 1598–1610.
(29) Nguyen, T. B.; Lehmann, J. Black carbon decomposition under varying water regimes. *Org. Geochem.* **2009**, *40*, 846–853.
(30) Harris, P. J. F.; Tsang, S. C. High-resolution electron microscopy studies of non-graphitizing carbons. *Phil. Mag. A—Physics Cond.*

Matter Structure Defects Mech. Prop. **1997**, *76*, 667–677.
(31) Cohen-Ofri, I.; Weiner, L.; Boaretto, E.; Mintz, G.; Weiner, S. Modern and fossil charcoal: aspects of structure and diagenesis. *J. Archaeol. Sci.* **2006**, *33*, 428–439.
(32) Nishimiya, K.; Hata, T.; Imamura, Y.; Ishihara, S. Analysis of chemical structure of wood charcoal by X-ray photoelectron spectroscopy. *J. Wood Sci.* **1998**, *44*, 56–61.
(33) Antal, M. J.; Grønli, M. The art, science, and technology of charcoal production. *Ind. Eng. Chem. Res.* **2003**, *42*, 1619–1640.
(34) Mochidzuki, K.; Soutric, F.; Tadokoro, K.; Antal, M. J.; Toth, M.; Zelei, B.; Varhegyi, G. Electrical and physical properties of carbonized charcoals. *Ind. Eng. Chem. Res.* **2003**, *42*, 5140–5151.
(35) Lu, L. M.; Sahajwalla, V.; Harris, D. Characteristics of chars prepared from various pulverized coals at different temperatures using drop-tube furnace. *Energy Fuels* **2000**, *14*, 869–876.
(36) Brodowski, S.; Amelung, W.; Haumaier, L.; Abetz, C.; Zech, W. Morphological and chemical properties of black carbon in physical soil fractions as revealed by scanning electron microscopy and energy-dispersive X-ray spectroscopy. *Geoderma* **2005**, *128*, 116–129.
(37) Kim, N. H.; Hanna, R. B. Morphological characteristics of Quercus variabilis charcoal prepared at different temperatures. *Wood Sci. Technol.* **2006**, *40*, 392–401.
(38) Ishimaru, K.; Vystavel, T.; Bronsveld, P.; Hata, T.; Imamura, Y.; De Hosson, J. Diamond and pore structure observed in wood charcoal. *J. Wood Sci.* **2001**, *47*, 414–416.
(39) Derenne, S.; Largeau, C. A review of some important families of refractory macromolecules: Composition, origin, and fate in soils and sediments. *Soil Sci.* **2001**, *166*, 833–847.
(40) Harris, P. J. F.; Burian, A.; Duber, S. High-resolution electron microscopy of a microporous carbon. *Phil. Mag. Lett.* **2000**, *80*, 381–386.
(41) Ban, L. L.; Crawford, D.; Marsh, H. Lattice-resolution electron-microscopy in structural studies of non-graphitizing carbons from polyvinylidene chloride (Pvdc). *J. Appl. Crystallogr.* **1975**, *8*, 415–420.
(42) Franklin, R. E. Crystallite growth in graphitizing and non-graphitizing carbons. *Proc. R. Soc. London Ser. A−Math. Phys. Sci.* **1951**, *209*, 196–217.
(43) Kirschbaum, M. U. F. The temperature-dependence of soil organic matter decomposition, and the effect of global warming on soil organic-C storage. *Soil Biol. Biochem.* **1995**, *27*, 753–760.
(44) Townsend, A. R.; Vitousek, P. M.; Desmarais, D. J.; Tharpe, A. Soil carbon pool structure and temperature sensitivity inferred using CO2 and (13) CO_2 incubation fluxes from five Hawaiian soils. *Biogeochemistry* **1997**, *38*, 1–17.
(45) Fierer, N.; Craine, J. M.; McLauchlan, K.; Schimel, J. P. Controls on microbial CO_2 production: a comparison of surface and subsurface soil horizons. *Ecology* **2005**, *86*, 320–326.
(46) Conant, R. T.; Steinweg, J. M.; Haddix, M. L.; Paul, E. A.; Plante, A. F.; Six, J. Experimental warming shows that decomposition temperature sensitivity increases with soil organic matter recalcitrance. *Ecology* **2008**, *89*, 2384–2391.
(47) Fang, C. M.; Smith, P.; Moncrieff, J. B.; Smith, J. U. Similar response of labile and resistant soil organic matter pools to changes in temperature. *Nature* **2005**, *433*, 57–59.
(48) Czimczik, C. I.; Trumbore, S. E. Short-term controls on the age of microbial carbon sources in boreal forest soils. *J. Geophys. Res.−Biogeosci.* **2007**, *112*, G03001.
(49) Reichstein, M.; Subke, J. A.; Angeli, A. C.; Tenhunen, J. D. Does the temperature sensitivity of decomposition of soil organic matter depend upon water content, soil horizon, or incubation time. *Global Change Biol.* **2005**, *11*, 1754–1767.
(50) Peterjohn, W. T.; Melillo, J. M.; Steudler, P. A.; Newkirk, K. M.; Bowles, F. P.; Aber, J. D. Responses of trace gas fluxes and N availability to experimentally elevated soil temperatures. *Ecol. Appl.* **1994**, *4*, 617–625.
(51) Lehmann, J.; Liang, B.; Solomon, D.; Lerotic, M.; Luizao, F.; Kinyangi, J.; Schäfer, T.; Wirick, S.; Jacobsen, C. Near-edge X-ray absorption fine structure (NEXAFS) spectroscopy for mapping nano-scale distribution of organic carbon forms in soil: Application to black carbon particles. *Global Biogeochem. Cycles* **2005**, *19*, GB1013.
(52) Nguyen, T. B.; Lehmann, J.; Kinyangi, J.; Smernik, R.; Riha, S. J.; Engelhard, M. H. Long-term black carbon dynamics in cultivated soil. *Biogeochemistry* **2008**, *89*, 295–308.
(53) Pierson, H. O. *Handbook of carbon, graphite, diamond and fullerenes properties, processing and applications*; Noyes Publications Park Ridge: New Jersey, 1993.
(54) Harris, P. J. F. New perspectives on the structure of graphitic carbons. *Critical Rev. Solid State Mat. Sci.* **2005**, *30*, 235–253.
(55) Fierer, N.; Allen, A. S.; Schimel, J. P.; Holden, P. A. Controls on microbial CO_2 production: a comparison of surface and subsurface soil horizons. *Global Change Biol.* **2003**, *9*, 1322–1332.
(56) Glaser, B.; Lehmann, J.; Zech, W. Ameliorating physical and chemical properties of highly weathered soils in the tropics with charcoal -a review. *Biol. Fert. Soils* **2002**, *35*, 219–230.
(57) Liang, B.; Lehmann, J.; Solomon, D.; Kinyangi, J.; Grossman, J.; O'Neill, B.; Skjemstad, J. O.; Thies, J.; Luizão, F. J.; Petersen, J.; Neves, E. G. Black carbon increases cation exchange capacity in soils. *Soil Sci. Soc. Am. J.* **2006**, *70*, 1719–1730.

ES903016Y